

# The structural and optical properties of $\gamma$ -FeOOH thin film grown with CBD method

O. ÖZDEMİR, F. MEYDANERİ\*, İ. A. KARİPER<sup>a</sup>

*Department of Metallurgy and Materials Engineering, Faculty of Engineering, Karabük University, 78050, Karabük, Turkey*

*<sup>a</sup>Department of Science Education, Education Faculty, Erciyes University, 38039, Kayseri, Turkey*

$\gamma$ -FeOOH thin films were produced by Chemical Bath Deposition (CBD) method at pH: 5 onto amorphous glass substrates. Structural properties of  $\gamma$ -FeOOH thin film were analyzed with X-ray diffraction (XRD). Chemical analysis and surface image of thin film were investigated with EDX, SEM, respectively. Optical properties were investigated via UV-VIS spectrophotometer.  $\gamma$ -FeOOH (lepidocrocite) crystal is orthorhombic structure and the XRD peak corresponding to the  $\gamma$ -FeOOH is enhanced to (1 1 1) plane. The allowed direct and allowed indirect optical band gaps ( $E_g$ ), optical transmission (T%), reflectivity (R%), absorption, refraction index (n), extinction coefficient (k), dielectric constant ( $\epsilon$ ) of the thin film were found to be 2.00 and 1.63 eV, 36.39 %, 24.86 %, 0.43, 2.98, 0.03 and 1.76, respectively.

(Received May 31, 2014; accepted July 10, 2014)

**Keywords:** CBD method, Crystal growth, Optical properties, pH, Microstructure

## 1. Introduction

Thin-film forms of iron oxides/oxyhydroxides are important materials for many industrial, scientific and technological applications such as photoelectrochemical solar cells for solar energy conversion, pigments, magnetic materials, catalysts and sensors [1-4]. Also, they are used as electrodes in Li batteries and super capacitors [5, 6]. Iron oxide thin films have been previously produced by various physical and chemical processes. Physical processes include dry processes such as molecular beam epitaxy (MBE) and sputtering [2, 5, 7]. Wet chemical processes such as the sol-gel method, liquid phase deposition (LPD), and the hydrothermal methods are tend to have little porosity and are coarse grained [8-11].

In general, the phase composition and properties of the precipitate depend on three parameters; oxidation of Fe (II) solution at various pH values, deposition time and the type of iron. As part of our research, we carried out experiments using the  $\text{FeCl}_3$ . Before presenting our results, it was investigated attention on some achievement studies in this field. The thin films have been previously produced by various physical and chemical processes. Lee et al. [12] investigated those magnetic properties of needle-like  $\alpha$ -FeOOH and  $\gamma$ -FeOOH nanoparticles. Yen et al. [13] investigated that crystallite size variation of nanosized  $\text{Fe}_2\text{O}_3$  powders during  $\gamma$  to  $\alpha$ -phase transformation. Antony et al. [14] investigated that electrochemical synthesis of lepidocrocite thin films on gold substrate. Streat et al. [15] investigated that hydrous ferric oxide as an adsorbent in water treatment. Therefore, in this paper, we purposed that producing oxide thin film by CBD method; investigating structural and optical properties depending on solution pH value, deposition time and

deposition temperature, and expanding the initial work that reported in previous publication.

## 2. Experimental procedure

### 2.1. Synthesis of thin films

$\text{FeCl}_3$ , distilled water ( $\text{H}_2\text{O}$ ), KOH, all of analytical grade, were used to produce the oxide thin film. A novel method was used to obtain the thin film. The method is a simple and inexpensive way to synthesize thin films of metal oxides, oxyhydroxides, oxychlorides and hydroxides. Firstly, 100 ml of 0.1 M  $\text{FeCl}_3$  solution was prepared into five beakers separately. Secondly, 7.0 ml KOH (10%) solution were added into the four of five beakers, respectively. The pH of chemical bath was determined to be pH=5 by using a pH meter (Lenko mark 6230N). Pre-washed and cleaned  $60 \times 20$  mm amorphous glass substrates were immersed into the prepared solutions, and the chemical bath was placed into oven. Finally, the oxide thin film on amorphous glass substrates was deposited keeping 24 h at a bath temperature of 65 °C. The reaction process for forming the thin films is considered as follows:



Many oxide derivatives may occur depending on the temperature, pH value, deposition time and pressure of the media. In this system, ions may have two functions: to slow down the hydrolysis rate of  $\text{Fe}^{+3}$  ions and to stabilize the oxygen-terminated crystal planes. We found that the most suitable pH value to grow along plane (1 1 1) is 5.

Lower pH (<5) or higher pH (>5) could not produce single phase due to their rapid dissolution, could lead to precipitates directly.

## 2.2. Characterizations of thin film

The crystal structure of the oxide thin film was confirmed by X-ray diffraction (XRD) with a  $\text{CuK}_{\alpha 1}$  radiation source (Rigaku RadB model,  $\lambda = 1.5406 \text{ \AA}$ ) over the range  $10^\circ < 2\theta < 90^\circ$  at a speed of  $3^\circ \text{ min}^{-1}$  with a step size of  $0.02^\circ$ . Chemical analysis of the thin film was performed with an EDX spectrometer attached to the SEM. The surface properties of the film were investigated using an EVO40-LEO computer controlled digital scanning electron microscope (SEM). The transmittance and absorbance measurements of the film were recorded by a Perkin Elmer UV/VIS Lambda 2S spectrophotometer (double-beam) at room temperature by placing an uncoated identical glass substrate in the reference beam in the wavelength range of 200-1100 nm. The film thickness was measured with a Veeco Multi Mode AFM (Controller=NanoScope 3D).

## 3. Results and discussion

### 3.1. Microstructural properties

Produced thin film was yellow-brown in color. The crystal structure and orientation of crystallization induced by the pH: 5 value of the chemical bath were determined with XRD measurement. Fig. 1 shows the diffraction pattern of the crystalline grown at pH: 5. Only one peak was observed at the diffraction angle of  $\sim 28.02^\circ$  for the  $\gamma$ -FeOOH thin film deposited at pH: 5. The diffraction pattern showed that the film grown in the present work is in a single-crystalline nature, in orthorhombic structure, and crystal orientation that enhanced to the (1 1 1) plane. The crystal orientation and the diffraction angle observed in literature for pH: 5 were obtained to be (1 2 0) plane and  $27.5^\circ$  [16], respectively. Unit cell parameters along the (1 1 1) plane were found to be  $a=10.6998 \text{ \AA}$   $b= 6.2135 \text{ \AA}$   $c= 3.9286 \text{ \AA}$ ,  $\alpha=\beta=\gamma=90^\circ$ . The Bragg's interplanar spacing for orthorhombic structure was calculated using the formula given below;

$$\frac{1}{d_{hkl}^2} = \frac{h^2}{a^2} + \frac{k^2}{b^2} + \frac{l^2}{c^2} \quad (2)$$

The observed (d) value of the Bragg's interplanar spacing was found to be  $3.171 \text{ \AA}$ . The grain size of the single-crystalline  $\gamma$ -FeOOH was calculated by X-Powder computer program versus higher intensity peak of XRD patterns using Debye Scherrer's formula,

$$D = \frac{K\lambda}{\beta \cos \theta} \quad (3)$$

where D is the grain size, K is a constant which is taken as 0.9,  $\lambda$  is the X-ray wavelength used,  $\beta$  is the angular line width at half-maximum intensity in radians and  $\theta$  is Bragg angle. Dislocation density ( $\delta$ ) was calculated using the formula given below:

$$\delta = \frac{1}{D^2} \quad (4)$$

where  $\delta$  is dislocation density which is defined as length of dislocation lines per unit volume of the crystal. The number of crystallites per unit area (N) is calculated by using the formula:

$$N = \frac{t}{D^3} \quad (5)$$

where t is the film thickness. The found results for some structural properties of  $\gamma$ -FeOOH thin film at pH: 5 are given in Table 1.

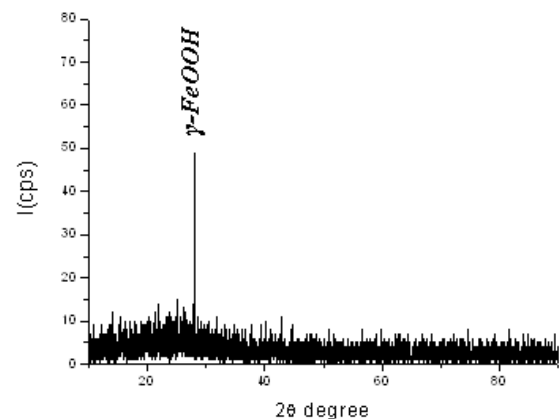


Fig. 1. X-ray diffraction pattern of single-crystalline  $\gamma$ -FeOOH thin film deposited on amorphous glass substrate at pH: 5.

Table 1. The grain size (D), dislocation density ( $\delta$ ), film thickness (t), optical band gap and the number of crystallites per unit area (N) values of FeOOH thin films at pH: 5.

| pH | t (nm) | D (nm) | Eg (eV) | $\delta \times 10^{-4}$ (lines/nm <sup>2</sup> ) | $N \times 10^{-3}$ (1/nm <sup>2</sup> ) |
|----|--------|--------|---------|--|---|
| 5  | 400    | 63.64  | 2.00    | 2.46   | 1.55                                    |

Scanning electron microscopy (SEM) was used to investigate surface properties of the film because the surface properties directly affect the optical properties of the films. The SEM image of the  $\gamma$ -FeOOH thin film produced at pH: 5 are presented in Fig. 2. The SEM analysis, as well as being in agreement with the XRD results, supplied additional experimental confirmation. As

can be seen from Fig. 2, the film is dense and have strong adherence to the substrates, and has a rough surface morphology. After small particles placed on the base, large particles were attached on them. There is no crack onto the surface of the film. The grain size results in an increase in the grain boundaries and the amount of defects in the structure. It is notable that accumulation of different heights and sizes in some areas of the film. These regions on the surface shows that the preferred growth areas by atoms. We think that the reason of the accumulation in different regions during the film formation is amorphous properties of used glass substrates and thermal differences between the substrate and the film. Good crystallization of the structure is due to the fact that the low rate of reaction and the nature of amorphous glass substrate. Besides, the dislocation density is very low depending on pH of the chemical bath, solution temperature (65 °C) and composition. This shows that after ions in solution are started to form of nucleation on amorphous glass, are gradually formed a precipitate. Here the effect of pH on particle growth was further investigated. These surface properties have strong effect on the optical properties of films. So, it was concluded that the surface properties of the film were improved for the film with single-phase grown at pH = 5. The EDX technique was used to estimate the composition of the thin film and is given in Fig. 3. In addition, Table 2 shows the percent of atomic ratios at pH: 5.

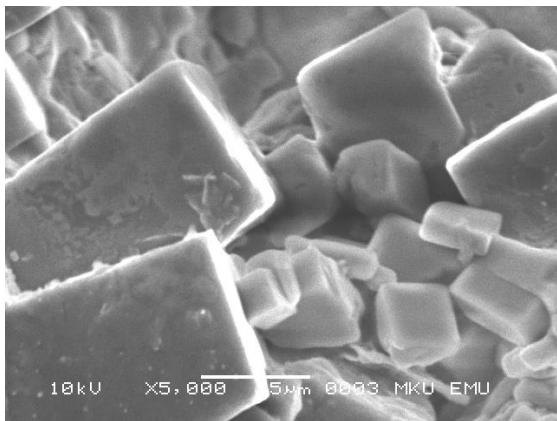


Fig. 2. SEM images of single-crystalline  $\gamma$ -FeOOH thin film deposited on amorphous glass substrate at pH:5.

Table 2. The change of percent atomic ratios.

| Element | Element % | Sigma % | Atomic % |
|---------|-----------|---------|----------|
| O       | 30.24     | 0.39    | 57.30    |
| Cl      | 14.03     | 0.20    | 11.99    |
| K       | 1.92      | 0.11    | 1.49     |
| Fe      | 53.81     | 0.41    | 29.21    |
| Total   | 100       | Total   | 100      |

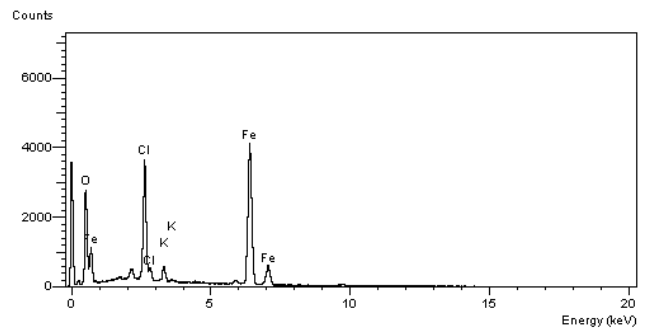


Fig. 3. The EDX analysis for  $\gamma$ -FeOOH thin film deposited on amorphous glass substrate.

### 3.2. Optical properties

In the present work, the optical properties such as transmittance, absorbance, reflection, refraction index, extinction coefficient and dielectric constant vary depending on crystallization and pH value. The thickness of the film was measured to be 400 nm in a  $10 \times 10 \mu\text{m}$  area with tapping mode by AFM. Transmission measurement was performed at room temperature in the range of 200-1100 nm to obtain information on the optical properties of  $\gamma$ -FeOOH thin film deposited on amorphous glass substrate at pH:5. The transmission and reflectance spectra of the film are shown in Fig. 4. The optical transmission was recorded to be 36.39 % in the visible region (550 nm) from UV-VIS spectra. In the visible region, the value of absorbance was determined to be 0.43 from UV-VIS spectra.

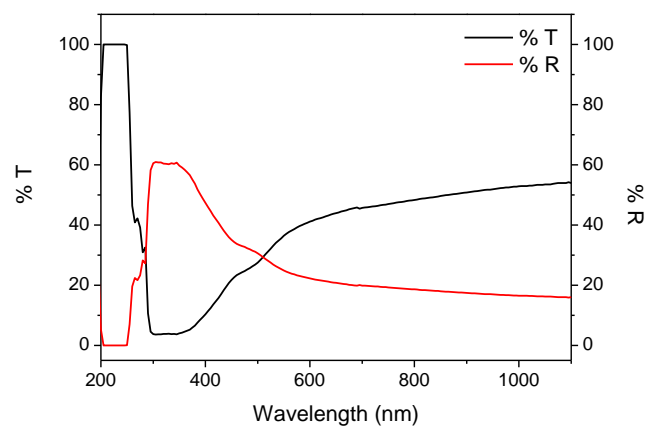


Fig. 4. The transmission and reflectance spectra of  $\gamma$ -FeOOH thin film.

The reflectivity (R) of  $\gamma$ -FeOOH thin film can be calculated using the transmittance (T) and absorbance (A) spectra from the expression [17]:

$$T = (1 - R)^2 \exp(-A) \quad (6)$$

The reflectivity ( $R$ ) of  $\gamma$ -FeOOH thin film was found to be 24.86 % in the visible region (550 nm).

Then, optical absorption coefficient, derived from transmittance and absorbance, is a function of photon energy and the presence of an absorption edge. In the visible region, the optical absorption coefficient was calculated to be of the order of  $10^5 \text{ cm}^{-1}$  (Fig. 5 (a)). The absorbance variation versus the wavelength of  $\gamma$ -FeOOH thin film is shown in Fig. 5 (b).

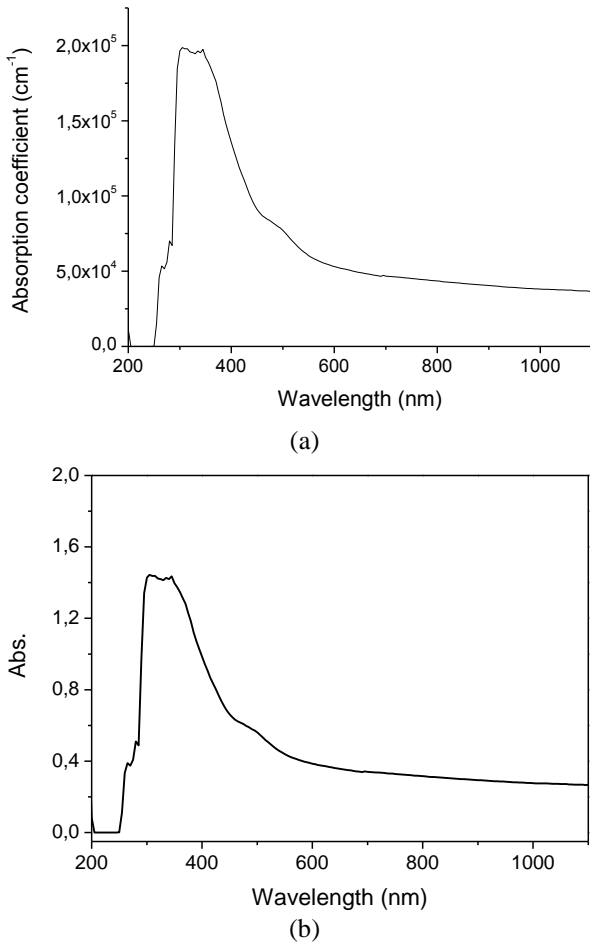


Fig. 5. (a) The absorption coefficient and (b) absorption changing versus the wavelength of the  $\gamma$ -FeOOH thin film.

After determining absorption coefficient, the value of optic band gap can be found. The region of higher values of  $\alpha$  that is  $\alpha > 10^4 \text{ cm}^{-1}$  correspond to transition between extended state in both valence and conduction bands while the lower values that is  $\alpha \leq 10^4 \text{ cm}^{-1}$  is the region where absorption present a rough exponential behavior. The absorption coefficient,  $\alpha$  determines how far into a material light of a particular wavelength can penetrate before it's absorbed. By using absorption coefficient, the value of band gap can be determined, by using the formula below [18],

$$(\alpha h\nu) = A(h\nu - E_g)^n \quad (7)$$

where  $\alpha$  is the absorption coefficient,  $(h\nu)$  is the photon energy,  $A$  is a coefficient and  $n$  value gets the values of  $1/2, 2$  for allowed direct and allowed indirect, respectively. The band structure of film is both direct and indirect transitions depending on its crystalline and type of material. To observe whether the film has direct or indirect gap, plots of  $(\alpha h\nu)^2$  versus  $(h\nu)$ ,  $(\alpha h\nu)^{1/2}$  versus  $(h\nu)$  were drawn, respectively. The plots are shown in Fig. 6. The straight-line was extrapolated to the energy axis at  $\alpha=0$ , to obtain band gap of the  $\gamma$ -FeOOH thin film. The plot of  $(\alpha h\nu)^2$  versus  $(h\nu)$  showed that the material has a direct band gap 2.0 eV while the plot of  $(\alpha h\nu)^{1/2}$  versus  $(h\nu)$  has an indirect band gap 1.63 eV. When absorbance spectra of the film is examined, it is notable that acting as an opaque material due to its absorption in the short wavelengths of the film, and material is color. At the same time, SEM images and the absorption values correct that film has very crystallinity and high absorbance value. The high absorbance of the film made them good materials for large area selective coating for photothermal conversion of solar energy.

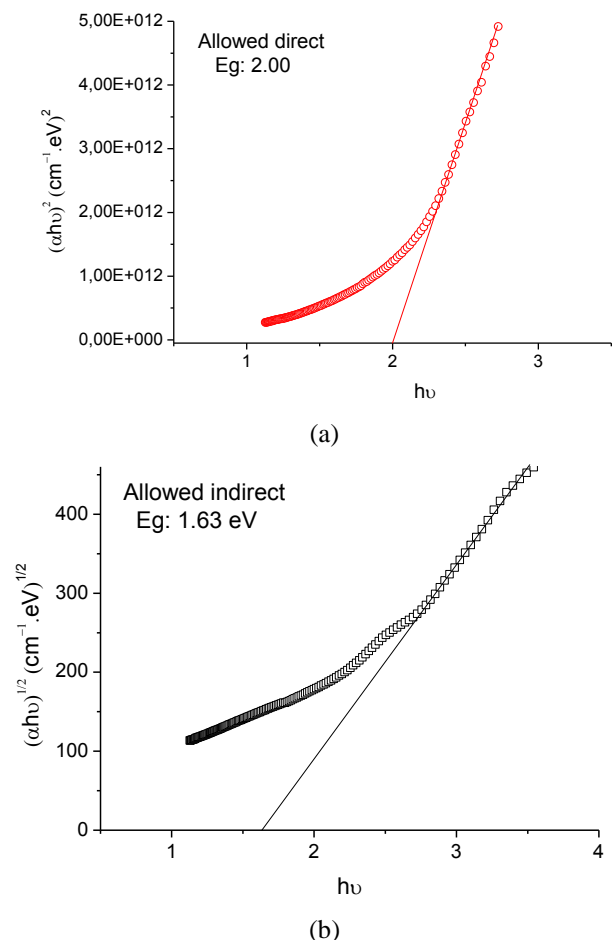


Fig. 6. The plots of a)  $(\alpha h\nu)^2$  versus  $(h\nu)$ , b)  $(\alpha h\nu)^{1/2}$  versus  $(h\nu)$  for the  $\gamma$ -FeOOH thin film.

The optical constants are parameters which characterize how matter will respond to excitation by an electromagnetic radiation at a given frequency. These

optical constants can be expressed as a complex dielectric function by the formula

$$\varepsilon = \varepsilon_1 + i\varepsilon_2 \quad (8)$$

or as a complex refractive index by the formula

$$n = n + ik \quad (9)$$

$$\varepsilon_1 = n^2 - k^2 \quad (10)$$

$$\varepsilon_2 = 2nk \quad (11)$$

The real part or refraction index ( $n$ ) defines the phase velocity of light in material. The imaginary part or extinction coefficient ( $k$ ) determines how fast the amplitude the wave decreases. Thus, the optical constants represent the optical properties of a material in terms of how an electromagnetic wave will propagate in that material.

Refraction index ( $n_r$ ) and extinction coefficient ( $k$ ) for the oxide thin films are given by the formulas [17]:

$$n_r = \frac{1+R}{1-R} + \sqrt{\frac{4R}{(1-R)^2} - k^2} \quad (12)$$

$$k = \frac{\alpha\lambda}{4\pi} \quad (13)$$

The refractive index and the extinction coefficient spectra of the  $\gamma$ -FeOOH thin film are shown in Fig. 7. In the visible region, the values of  $n_r$  and  $k$  were obtained to be 2.98 and 0.03, respectively. The dielectric constant versus the wavelength for  $\gamma$ -FeOOH thin film is shown in Fig. 8, and the value of dielectric coefficient was calculated to be 1.76. The extinction coefficient of a material depends on directly absorption characteristics of the material. These results also are supported transmission and absorption spectra of the film. Also, high-index materials are used to make the filters and mirrors used in lasers with special reflecting by optimal designs. The optical properties of  $\gamma$ -FeOOH thin film in the literature are not. Therefore, the calculated/determined results in the present work did not compare.

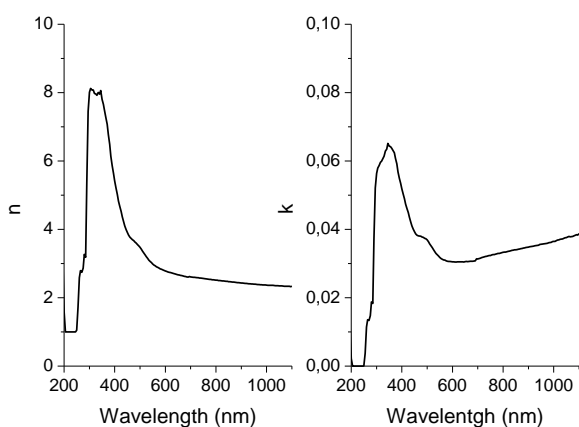


Fig. 7. The refractive index and the extinction coefficient spectra of  $\gamma$ -FeOOH thin film.

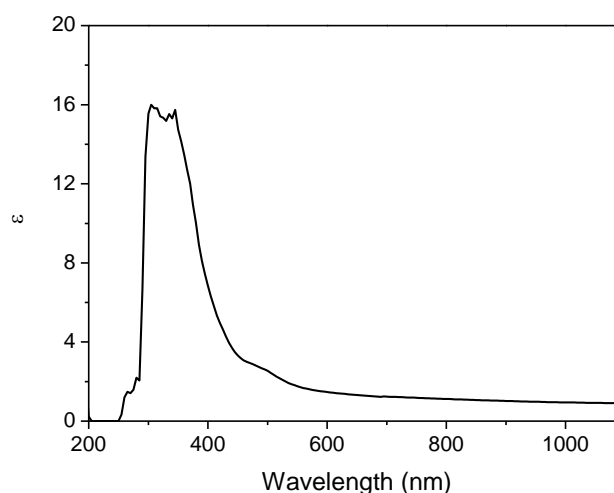


Fig. 8. The dielectric constant versus the wavelength of the  $\gamma$ -FeOOH thin film.

#### 4. Conclusions

$\gamma$ -FeOOH thin films were produced by CBD technique at pH: 5 onto amorphous glass substrates. Structural and optical properties of the  $\gamma$ -FeOOH thin film were investigated. Crystal structure of  $\gamma$ -FeOOH was found to be orthorhombic. The XRD peak corresponding to the  $\gamma$ -FeOOH was enhanced to (1 1 1) plane. The optical transmission ( $T$  %), reflectivity ( $R$  %), absorption coefficient ( $\alpha$ ), refraction index ( $n_r$ ), extinction coefficient ( $k$ ), dielectric constant ( $\varepsilon$ ) of the film were found to be, 36.39 %, 24.86 %, 0.43, 2.98, 0.03 and 1.76, respectively.

#### Acknowledgement

This work was supported by TUBİTAK-2209 (A 2012/1) Project, authors would like to thank to TUBİTAK-2209 Project Unit for their financial support.

#### References

- [1] V. A. Hiremath, A. Venkataraman, Bull. Mater. Sci. **26**, 391 (2003).
- [2] E. L. Miller, D. Paluselli, B. Marsen, R. E. Rocheleau, Thin Solid Films, **466**, 307 (2004).
- [3] B. Pal, M. Sharon, Thin Solid Films **379**, 83 (2000).
- [4] S. S. Kulkarni, C. D. Lokhande, Mater. Chem. Phys. **82**, 151 (2003).
- [5] J. Sarradin, A. Guessours, M. Ribes, J Power Sources **62**, 149 (1996).
- [6] K. W. Chung, K. B. Kim et al. J The Electrochemical Society, **152**, C560 (2005).
- [7] Y. Gao, S. A. Chambers, J Cryst Growth, **174**, 446 (1997).
- [8] N. Özer, F. Tepehan, Sol Energy Mater Sol Cells, **56**, 141 (1999).

- [9] A. A. Akl, *Appl Surf Sci* **233**, 307 (2004).
- [10] S. Deki, N. Yoshida, Y. Hiroe, K. Akamatsu, M. Mizuhata, A. Kajinami, *Solid State Ionics* **151**, 1-9 (2002).
- [11] Q. W. Chen, Y. T. Qian, H. Qian, Z. Y. Chen, W. B. Wu, Y. H. Zhang, *Mater Res Bull*, **30**, 443 (1995).
- [12] G. H. Lee, S. H. Kim, B. J. Choi, S. H. Huh, Y. Chang, B. Kim, J. Park, S. J. Oh, *J Korean Phys Soc* **45**, 1019 (2004).
- [13] F. S. Yen, W. C. Chen, J. M. Yang, C. T. Hong, *Nano Lett* **2**, 245 (2002).
- [14] H. Antony, S. Peulon, L. Legrand, A. Chausse, *Electrochim Acta*, **50**, 1015 (2004).
- [15] M. Streat, K. Hellgardt, N. L. R. Newton, *Process Saf Environ*, **86**, 1 (2008).
- [16] R. Paterson, H. Rahman, *J Colloid Interf Sci*, **97**, 423 (1984).
- [17] S. Hamada, E. Matijevi, *J Chem Soc, Faraday Trans I*, **78**, 2147 (1982).
- [18] T. Müller, Chapter 3, Logos Verlag Berlin GmbH, pp. 6 (2009).

---

\*Corresponding author: meydaneri@yahoo.com